Received: 9 April 2024 | Revised: 28 May 2024 | Accepted: 31 May 2024

DOI: 10.1002/pip.3829

RESEARCH ARTICLE

PROGRESS IN PHOTOVOLTAICS WILEY

Intrinsic performance loss rate: Decoupling reversible and irreversible losses for an improved assessment of photovoltaic system performance

Hugo Quest [1,2] | Christophe Ballif [1,3] | Alessandro Virtuani [3]

[1]École Polytechnique Fédérale de Lausanne (EPFL), Institute of Electrical and Micro Engineering (IEM), Photovoltaics and Thin-Film Electronics Laboratory, Neuchâtel, Switzerland

[2]3S Swiss Solar Solutions AG, Gwatt (Thun), Switzerland

[3]Swiss Centre for Electronics and Microtechnology (CSEM), Sustainable Energy Centre, Neuchâtel, Switzerland

Correspondence
Hugo Quest, EPFL STI IEM PV-LAB, Rue de la Maladière 71b, CP 526, CH-2002 Neuchâtel, Switzerland.
Email: hugo.quest@epfl.ch

Funding information
Swiss Federal Office of Energy (SFOE), Project ASSURed PV, contract 502408-01.

Abstract

Solar electricity is set to play a pivotal role in future energy systems. In view of a market that may soon reach the terawatt (TW) scale, a careful assessment of the performance of photovoltaic (PV) systems becomes critical. Research on PV fault detection and diagnosis (FDD) focuses on the automated identification of faults within PV systems through production data, and long-term performance evaluations aim to determine the performance loss rate (PLR). However, these two approaches are often handled separately, resulting in a notable gap in the field of reliability. Within PV system faults, one can distinguish between permanent, irreversible effects (e.g. bypass diode breakage, delamination and cell cracks) and transient, reversible losses (e.g. shading, snow and soiling). Reversible faults can significantly impact (and bias) PLR estimates, leading to wrong judgements about system or component performance and misallocation of responsibilities in legal claims. In this work, the PLR is evaluated by applying a fault detection procedure that allows the filtering of shading, snow and downtime. Compared with standard filtering methods, the addition of an integrated FDD analysis within PLR pipelines offers a solution to avoid the influence of reversible effects, enabling the determination of what we call the intrinsic PLR (i-PLR). Applying this method to a fleet of PV systems in the built environment reveals four main PLR bias scenarios resulting from shading losses. For instance, a system with increasing shading over time exhibits a PLR of −1.7%/year, which is reduced to −0.3%/year when reversible losses are filtered out.

KEYWORDS
degradation, fault detection and diagnosis (FDD), performance loss rate (PLR), reliability, reversible losses, shading

1 | INTRODUCTION

1.1 | Exponential growth and decay?

Following the rapid expansion of the photovoltaic (PV) systems market and advancements in cell technology, solar power is more than ever promoted as one of the safest, cleanest and most abundant energy sources. Global cumulative capacity increased by 1 order of magnitude in the last 10 years, reaching the 1 TWp milestone in 2022,[1] and is predicted to more than double to 2.3 TWp in 2025.[2,3] Yearly installed capacity is growing exponentially, with an additional 240 GWp in 2022.[4] This value should further increase to about 3 TWp per year in order to meet the 2050 target of 70 TWp of global capacity[5]—the market is therefore at the cusp of TW-scale growth. This also follows a 90% decrease in cost of solar between 2009 and 2021.[2] With this expected increase in PV deployment, along with the growing amount of novel cell technologies entering the market,[6–9] module and system reliability are more than ever central topics in the field.[10–12] It has arguably never been more important and relevant to have a robust understanding of long-term performance loss mechanisms in PV, with new degradation and failure modes potentially arising from the changing bill of materials (BOM), module configurations and varying environmental factors.[13–18] Reliability is also crucial for any PV technology's commercial viability, with target lifetimes increasing to 40 + years.[19,20] New accelerated testing and field monitoring methods capable of dealing with the rapid market expansion and upscaling should be developed with a focus on data-based solutions to leverage the increasing flow of PV monitoring data from inverters and smart-metres. Digitalisation is therefore key in guiding operation and maintenance (O&M) activities and reducing their cost, extending PV system lifetime, and consequently improving system performance and energy yield, thus reducing the levelised cost of electricity (LCOE).

1.2 | Performance loss rate (PLR) and PV system monitoring: A brief review

PV system performance is most commonly assessed with the PLR metric. While certain key performance indicators (KPI), for example, the performance ratio (PR), are clearly defined in standards such as the IEC 61724-1:2021, there is still no consensus for the definition of the PLR.[21–24] The most common misconception observed in literature is the commutable use of the terms degradation rate (Rd) and PLR: In general, PLR refers to system-level performance losses, including both reversible (e.g. soiling, shading and snow) and irreversible effects, such as module-level degradation. In this work, the PLR is defined as the change in annualised PR relative to the first year, following the definition of Deceglie et al.[23] The degradation rate (Rd), defined as the rate at which a PV module efficiency decreases over time, is therefore a component of the PLR.

An additional layer of complexity in the PLR is the abundance of methods and variations of the PLR metric.[22,25,26] Although the general steps to compute the PLR are similar in all cases, the statistical model to extract the final reported value can vary significantly, leading to large differences in results as well as complex uncertainty assessments. Lindig et al. provide a succinct summary of the state of the art and best practises for PLR calculations.[22] Common PLR analysis pipelines include (i) input data quality evaluation, (ii) data filtering, (iii) performance metric selection, (iv) aggregation and (v) PLR calculation using statistical models. However, there are no uniform approaches to reliably calculate the PLR, as concluded by the International Energy Agency (IEA) Photovoltaic Power System Program (PVPS) Task 13 report.[21] Instead, an ensemble approach is deemed the most reliable calculation method, which consists in comparing multiple analysis pipelines (varying the filtering approaches and statistical models) and taking the mean inlier estimate. In this work, the Year-on-Year (YoY) methodology is used as the statistical model, as it is considered one of the most reliable regression analysis methods for long-term performance assessment of PV systems[27,28] and is implemented directly in PLR analysis pipelines such as *RdTools*.[29] Other statistical models include least-squares linear regression (LR),[17] seasonal trend decomposition using LOESS (locally estimated scatterplot smoothing) (STL),[18,30] statistical clear-sky fitting (SCSF)[31,32] and various nonlinear models such as Facebook Prophet (FBP)[33,34] and piece-wise regression.[35,36]

Lindig et al. also emphasise other challenges and opportunities for performance loss estimations, such as the potential actionable insights that can be gained through a component break-down analysis of the PLR. Detailed knowledge of individual performance losses could inform operations and maintenance (O&M) activities and reduce noise in the PLR value. More recently, Deceglie et al. further highlight the importance of distinguishing recoverable and nonrecoverable losses,[23,37] which have implications in the O&M and module technology and operational environments, respectively. This work aims to answer this open question, providing a method to filter reversible and irreversible performance losses.

1.3 | Loss factors and degradation modes (DMs)

In this work, a fault is used as the general term for any effect causing module power loss or safety issues.[38–42] Within PV system faults, certain categorisations are useful to further distinguish between a permanent, irreversible effect, known as a DM,[43] or transient, reversible losses, hereby called a loss factor (LF).[44] Importantly, as well as causing intermittent output losses, in the long run, LFs may lead to DMs, causing irreversible damage. For example, a typical LF is recurring shading, which causes performance loss and may evolve into hot spots, potentially leading to long-term damage such as delamination and glass cracks.[45–48] There is therefore a complex interplay between these LFs, which can act as stressors on multiple system components and levels, leading to further system faults.[11] Figure 1A shows the decomposition of the PLR between DMs and LFs, with example fault types.

Typically, PV manufacturer warranties state that module performance should remain above 80% of nominal power after 25 years,

which translates to module degradation below 0.8%/year, assuming a linear trend. Figure 1B (adapted from Köntges et al.[49]) shows typical performance loss scenarios with the impacting DMs. To ensure modules last long and continue to perform above the warranty levels, it is vital to avoid early and midlife degradation which would cause severe, irreversible power loss. However, as discussed above, when considering data-based approaches to quantify module or system performance loss, LFs and external faults are embedded in the PLR metric. This can cause unexplained high values of performance loss, for example, due to evolving and growing losses over time. In particular, PV systems in the built environment are often subjected to recurring shading events and high temperature working conditions,[50–52] which can therefore have both direct effects on their long-term performance or cause negative bias in the performance trend analyses. While high temperatures are relatively well understood and studied, with the IEC TS 63126 directly addressing solutions and modification in PV installations with high temperatures,[53,54] shade-induced degradation is not yet fully understood.[45] With routine shading events being prevalent in these types of systems, bypass diode (BPD) activation is expected to occur more frequently, which could lead to accelerated degradation due to the heat dissipation and potential damage to the BPD or nearby components.[55–57]

1.4 | The case of PV in the built environment

The rapid PV market expansion will drive a growth in building-integrated and building-applied PV systems (BIPV and BAPV, respectively).[58–60] In particular, BIPV systems are dual purpose, as they not only produce energy but also provide construction functions within building skins, thus reducing the cost of refurbishment and renovation of existing buildings. However, BIPV systems are known to have unique and variable operating environments, as they are often subjected to elevated operating temperatures and regular shading, demanding special attention to the module and system design.[61–63] Along with the potential short-term reduction of energy yield, these conditions risk affecting the long-term performance of such systems, through accelerated degradation mechanisms or early failures.[45,64] It is therefore vital to have a clear understanding of the operating conditions and additional stresses for PV in the built environment, with tailored monitoring solutions.[45,61] Thus, the methods developed in this work are applied to a fleet of BIPV and BAPV systems in Switzerland, in order to gain insights in their long-term operation and how the identified LFs (especially shading) affect their performance and reliability. The applicability of these findings to larger PV installations is described in the discussion section.

1.5 | Proposed integrated solution

Within this context, this work proposes a novel method to evaluate the PLR of PV systems by applying a fault detection and diagnosis (FDD) procedure that allows the filtering of shading, snow and downtime losses. Compared with standard filtering methods, which do not reflect the intrinsic system health due to the inherent inclusion of reversible losses in the data, the addition of FDD analysis within PLR pipelines offers a solution to avoid the influence of such reversible effects, enabling the determination of what we call the i-PLR.

This work applies the developed Fault Detection and Diagnosis Algorithm (FDDA) to BIPV systems, in combination with their long-term performance assessments. This paper is structured as follows: Section 2 describes the methodology, focusing first on the FDDA, and then the PLR assessment. Section 3 describes the results, which are are divided in three parts: (i) example daily profiles of the identified fault types; (ii) a case study of a BIPV system, where the full i-PLR pipeline is applied and an on-site analysis is conducted to validate and confirm the identified issues and (iii) fleet analysis results, highlighting the main findings in terms of patterns in LFs and PLRs. Section 4

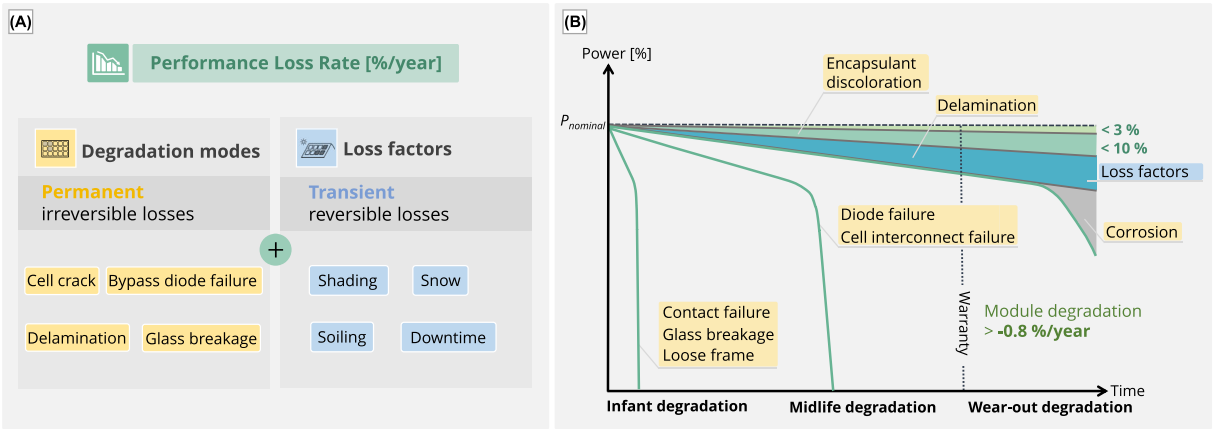

FIGURE 1 (A) Two components of the performance loss rate (PLR): degradation modes and loss factors. (B) Typical performance loss scenarios for PV modules, adapted from Köntges et al.[49] A few typical degradation modes are highlighted in yellow, and loss factors in blue—varying stressors over time can impact the performance trend. The goal of this work is to decouple these various hidden effects from the performance trend.

discusses the results within the broader PV context, highlighting both innovations and limitations. Finally, Section 5 concludes on the main outcomes and future work.

2 | METHODS

The PLR should be understood as the sum of reversible and irreversible performance loss effects in PV systems, and the goal of this work is to decouple reversible loss effects from the metric in order to better reflect PV system long-term performance. To this end, two main analysis steps are required: (i) a fault detection step to identify reversible effects and (ii) a PLR estimation step including fault-type filtering.

2.1 | Developed fault detection algorithm

The primary goal of the developed fault detection algorithm is to identify LFs (reversible faults) within the PV system data. Building upon the previous work of Fairbrother et al.,[45] an algorithm capable of distinguishing six operating conditions is developed, based on the analysis of string-level DC outputs compared with simulated outputs. The general analysis pipeline is described here, following the flowchart logic shown in Figure 2:

1. **Data acquisition.** The required data for the algorithm are the following: (i) PV system DC outputs (current, voltage and power), PV system metadata (system tilt, orientation, DC size/capacity) and site-specific meteorological data (global, direct and diffuse irradiance). In this case, satellite-based irradiance data are used.[65]
2. **Data preprocessing.** The PV system data are filtered and cleaned before running the fault detection analysis. A filter checks for outliers in the DC power data, based on the known system capacity ($0 < P_{DC} \leq 1.5 \cdot P_{STC}$, with P_{DC} [W] the DC power and P_{STC} [Wp] the string or system capacity). Plane-of-array irradiance is also calculated at this step using a transposition model based on system orientation and tilt (in this work, the Hay–Davies model is used[66]).
3. **PV output modelling.** The *pvlib* Python library is used to simulated DC outputs (current, voltage and power).[67] The Sandia Array Performance Model (SAPM) is used as a basis for the modelling.[68] Specifically, the *ModelChain* class is used to create a digital twin of the studied system or string, with the Faiman temperature model.
4. **Day type classification.** The irradiance data are used to distinguish four types of daily weather (cloudless, nearly cloudless, cloudy, overcast), which is used as an input for the fault classification. The day type classification model is based on a Support Vector Machine (SVM) classification model trained on over 10 years of labelled meteorological data, using the direct normal irradiance (DNI) as input parameter for training.[69] Alternatively, the *detect_clearsky* function from *pvlib* can be used to identify time steps with clear-sky conditions.
5. **Fault classification.** The comparison of the actual and simulated DC outputs (specifically the combination of voltage and current), along with the day type information, allows for the identification of six distinct operating conditions. For each analysed day, statistical thresholds based on the daily standard deviations of the voltage and current are defined around the simulated outputs, and the FDDA checks whether the actual DC values fall within or outside the defined boundaries, as detailed in.[45] The distinguished faults are described below, and example daily profiles are given for each fault type in section 3:

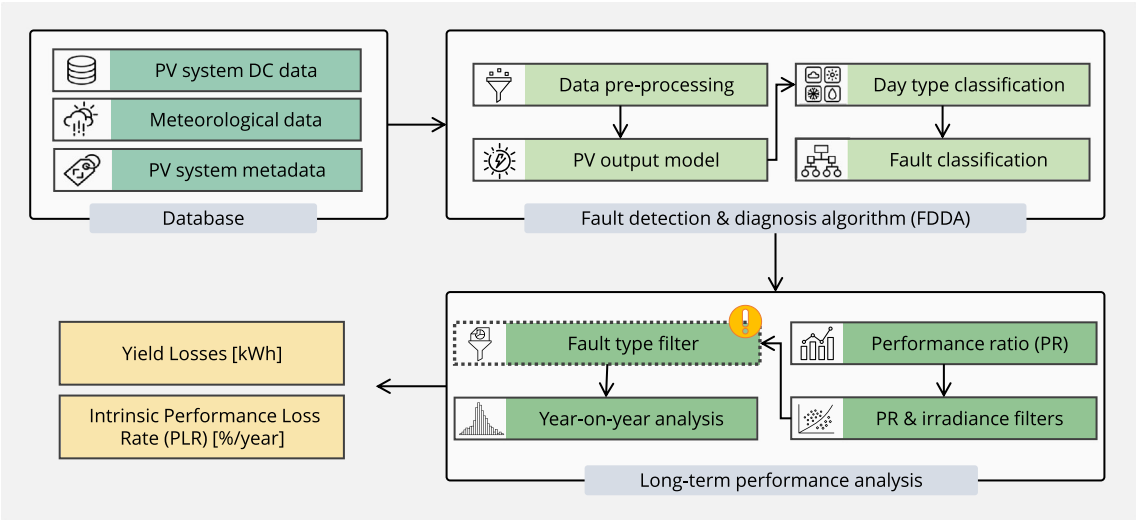

FIGURE 2 Simplified flowchart of the developed fault detection and diagnosis algorithm (FDDA) and long-term performance assessment. The outputs of the FDDA are used to filter the loss factors and compute corresponding yield losses, leading to the definition of the intrinsic PLR (i-PLR) reflecting system degradation.

- **F0|Normal**: Represents the normal performance state, with no faults or anomalies detected. The voltage and current are within the defined boundaries.
- **F1|Snow**: Snow-related losses, generally characterised by a drop in current and/or lower voltage due to the activation BPDs or inactive modules, depending on the snow cover. Inhomogeneous snow cover will yield current losses and low voltage, while homogeneous snow can cause downtime (if snow if opaque) or high voltage and low current (if there is low light transmittance through the snow). Specifically, snow is detected if $(I_{DC} < 0.1 \cdot I_{sim})$, where I_{DC} [A] is the DC current and I_{sim} [A] the simulated DC current.
- **F2|Cloudy**: Transient shading faults due to passing clouds, causing mismatches in current and/or voltage. These faults can be characterised by drops in voltage and current in cloudy or partially cloudy conditions, where short-term and nonrecurring shading from clouds is expected. The mismatch occurs mostly due to the uncertainty in the satellite-based weather data, which has limited accuracy at 10–15 min time steps. These faults are detected only for cloudy or overcast days, based on the day type classification step, where voltage or current are below the defined thresholds: $(V_{DC} < V_{sim} - 2 \cdot \sigma_V)$ and $(I_{DC} < I_{sim} - 0.5 \cdot \sigma_I)$, where V_{DC} [V] is the DC voltage, V_{sim} [V] the simulated DC voltage, σ_V the daily standard deviation of DC voltage used to define the fault detection thresholds and σ_I the daily standard deviation of DC current. The higher weight applied to the voltage threshold reflects the lower variability of DC voltage in a given day, while a lower weight is applied to current as the daily standard deviation is inherently higher (directly correlated to the irradiation variations during the day).[45]
- **F3|Shading (BPD activation)**: BPD activation is a common LF in BIPV systems, as it occurs during shading events due to external elements. The voltage will decrease abruptly due to the bypassed module sections with partial shading. These faults are only detected during cloudless or nearly cloudless days (to avoid the uncertainty of partial shading in diffuse light conditions), when $(V_{DC} < V_{sim} - 2 \cdot \sigma_V)$. These faults are mostly recurring shadowing, due to trees, chimneys or building elements, which cause periodic shadows. The shading pattern usually evolves with a seasonal trend due to solar angle dependencies.
- **F4|Shading (MPPT)**: Similar to F3, although their data fingerprint is different. Partial shading can cause mismatches in the current output of the string due to modules receiving varying irradiance levels, causing multiple steps in the I–V characteristic of the string. Depending on the inverter type, the maximum power point tracking (MPPT) algorithm can adjust the voltage to higher values, with limited current defined by the shaded module(s). In such conditions where there are multiple MPPs, tracking algorithms that start scanning from the open-circuit voltage can therefore remain at high voltages with limited current: $(V_{DC} > V_{sim} + 2 \cdot \sigma_V)$ and $(I_{DC} < I_{sim} - 0.5 \cdot \sigma_I)$.
- **F5|Downtime**: State of downtime or data loss, where PV strings and/or data logging are disconnected or malfunctioning. This can occur in extreme events, for example, during lightning or hail storms, or can be linked to connection or server issues, broken fuses or simply offline inverters. The fault is detected when the DC parameters (current, voltage and power) are missing or equal to 0 during daylight.

2.2 | Long-term performance and i-PLR

Once the FDD step identifies the time steps during which PV systems experience LFs, the next step of the analysis is the determination of the PLR (see Figure 2). The main steps for computing the PLR proposed by the IEA PVPS Task 13 experts[24] consist of (i) input data cleaning, (ii) data filtering, (iii) performance metric selection, (iv) aggregation and (v) use of a statistical modelling method to calculate the PLR. However, there is no consensus on a single PLR computations strategy, with possible variations in almost all calculation steps. Thus, data quality and data-related uncertainties play a significant role in the PLR values, which adds a layer of complexity in the determination of a single, robust quantification of a system's health.[22,70–73] Although there is no standardised approach, the year-on-year (YoY) methodology is often deemed the most robust regression analysis method for long-term performance assessment of PV systems.[27,74] It relies on the comparison of normalised yields through subsequent years. This results in a statistical distribution of PLR values, where the median is usually taken as the system PLR. The analysis steps are generally as follows: Firstly, the string-level PV system yield is normalised using the PR, defined as the quotient between the system's final and reference yield. Following the IEC 61724-1 guidelines, the PR can be further adjusted for temperature dependence and is denoted PR′ as follows:

$$PR' = \frac{\left(\sum_k P_{mp,k} \cdot \tau_k\right)}{\left(\sum_k \frac{(C_{k,25^\circ C} \cdot P_0) \cdot G_{i,k} \cdot \tau_k}{G_{i,ref}}\right)} \quad (1)$$

$$C_{k,25^\circ C} = 1 + \gamma \cdot (T_{mod,k} - 25^\circ C) \quad (2)$$

Where for the k time steps with recording interval τ, P_{mp} [W] is the measured DC power at MPP, P_0 [Wp] the rated power, $G_i\left[\mathrm{Wm^{-2}}\right]$ the measured in-plane irradiance, $G_{i,\mathrm{ref}} = 1000\,\mathrm{Wm^{-2}}$ the irradiance at which P_0 is determined (STC), $C_{k,25^\circ C}$ the power rating temperature adjustment factor, T_{mod} [°C] the module temperature and γ [%/°C] the relative maximum power temperature coefficient. For the standard PR, the temperature correcting term is set to 1.

In this work, the standard PR is used (no temperature correction). The next step involves filters which are applied to remove outliers and improve data quality (using the data at 15 min time steps)—an irradiance filter to remove extreme irradiance conditions (< 100 W m^{-2} or > 1250 W m^{-2}) and a PR filter with low and high thresholds of 0.3 and 1.2, respectively (removing extreme shading mismatches and irradiance peaks due to cloud reflections). The novelty compared with standard PLR pipelines is then introduced with the fault type filter.

This step aims to remove all influence of reversible faults, that is, LFs, from the system data, making use of the prior FDDA results. To do so, all time steps that are detected in operating conditions F1–F5 are filtered out, leaving only the F0 state which represents normal operation, essentially decoupling the reversible losses from the PV system data. The PR is then aggregated to daily averages, and a final clear-sky filter is applied (based on the day type classification step), removing cloudy or overcast days.[69] The PR values are then renormalised to the first year of operation data in order to compute the annualised performance loss. Finally, the PLR can be computed using the YoY regression analysis, which results in a histogram of PLRs, of which the median value is considered as the final system PLR. Specifically, instances of PLRs (denoted YoY) are computed by comparing the PR from 1 year to the next:

$$YoY = \frac{PR^d_{\text{year i}} - PR^d_{\text{year i}-1}}{\Delta t[\text{years}]} \quad (3)$$

where $PR^d_{\text{year i}}$ is the daily PR on a given day in year i, $PR^d_{\text{year i}-1}$ the daily PR of the prior year and Δt the difference between the two points in years. Repeating this for all PR values yields a distribution of YoY comparisons, of which the median is selected as the final PLR. When the fault type filtering is applied, this value is what we define as the i-PLR, reflecting the intrinsic PV system degradation. Removing the fault type filtering step would yield the standard PLR, which can then be compared with the intrinsic value to gain insights on the impact of LFs on the PLR.

2.3 | Understanding and assessing uncertainties

The subject of uncertainty should also be discussed when computing metrics such as the PR and PLR. There are two main components to the uncertainty: (i) analytical uncertainty, associated with the limitations inherent in the measurement instrument or method itself, that is, the uncertainty of the satellite- or ground-based irradiance measurements, which translates to a measurement uncertainty in the PR, and (ii) statistical uncertainty, associated with the variability observed in a set of measurements, that is, the uncertainty related to the statistical tool used to evaluate the PLR. For the first component, minimising the uncertainty can be achieved by using well maintained and calibrated ground sensors. However, access to pyranometer data is often not possible for smaller commercial or residential PV systems, and satellite-derived data were found to be a valid alternative when ground measurements are not available.[75] Regarding the statistical uncertainty, the exact methods depend on the statistical model chosen for the PLR estimation. The general formula to determine the 95% confidence interval (CI) is as follows:

$$U_{PLR} = k \cdot u_{PLR} \quad (4)$$

where U_{PLR} is the expanded uncertainty, k the coverage factor ($k = 1.96$ for 95% CI) and u_{PLR} the standard uncertainty derived from the measurement results. In the case of LR models, u_{PLR} is determined from the variance of the linear model coefficients.[22] For the YoY method applied in this work, bootstrap resampling of the probability density function of individual YoY instances is used to determine the uncertainty.[76]

Importantly, the CIs of PLR measurements need to be reported clearly. The uncertainty of PLR assessments is inconsistently shared in current literature (often only the median value is published), which leads to further misunderstanding of the metric. Statistical significance is especially crucial for the PLR when values are compared, for example, examining the performance of different PV technologies or climates. Without clear CIs, no conclusion can be made on the statistical significance of results.

3 | RESULTS

3.1 | Identified fault types and LFs

Figure 3 shows example daily profiles of DC current I_{DC} [A] and voltage V_{DC} [V], with statistical thresholds based on simulated model outputs I_{sim} and V_{sim} shown as shaded areas. Heat maps below each fault type example show detected faults (at 15 min. time steps) as well as relative current loss [%], which is a quantification of the relative difference between the simulated and actual currents. These fault examples are extracted from different PV system string, hence the variations in current and voltage axis ranges. The following comments can be made for each fault type:

- **F0|Normal**: Voltage and current are both within the defined thresholds. This example shows a typical clear-sky day for a good performing system, with the expected gradual voltage drop due to increasing irradiance and thus operating temperature during the day.
- **F1|Snow**: Extremely low current and reduced voltage indicate partial coverage of modules with opaque snow, causing the limited module(s) to dictate current behaviour, and BPD activation causing the voltage drop.
- **F2|Cloudy**: Typical cloudy or overcast days see a voltage curve which does not diminish in the middle of the day like in the example of F0, as the temperature is more stable. Here, a drop in voltage during short-term inhomogeneous irradiance conditions is observed in the morning, likely due to a mismatch between the satellite-based irradiance data and the actual observed irradiance.
- **F3|Shading (BPD activation)**: A 50% drop in voltage is observed in the afternoon, indicating BPD activation due to some form of partial shading in the string.
- **F4|Shading (MPPT)**: In this case of irradiance mismatch, the maximum power point tracker (MPPT) adjusted the voltage and current to the local instead of global MPP, causing a limited current and high yield losses.
- **F5|Downtime**: The system disconnected for around 30 min in the evening, causing a gap in the data.

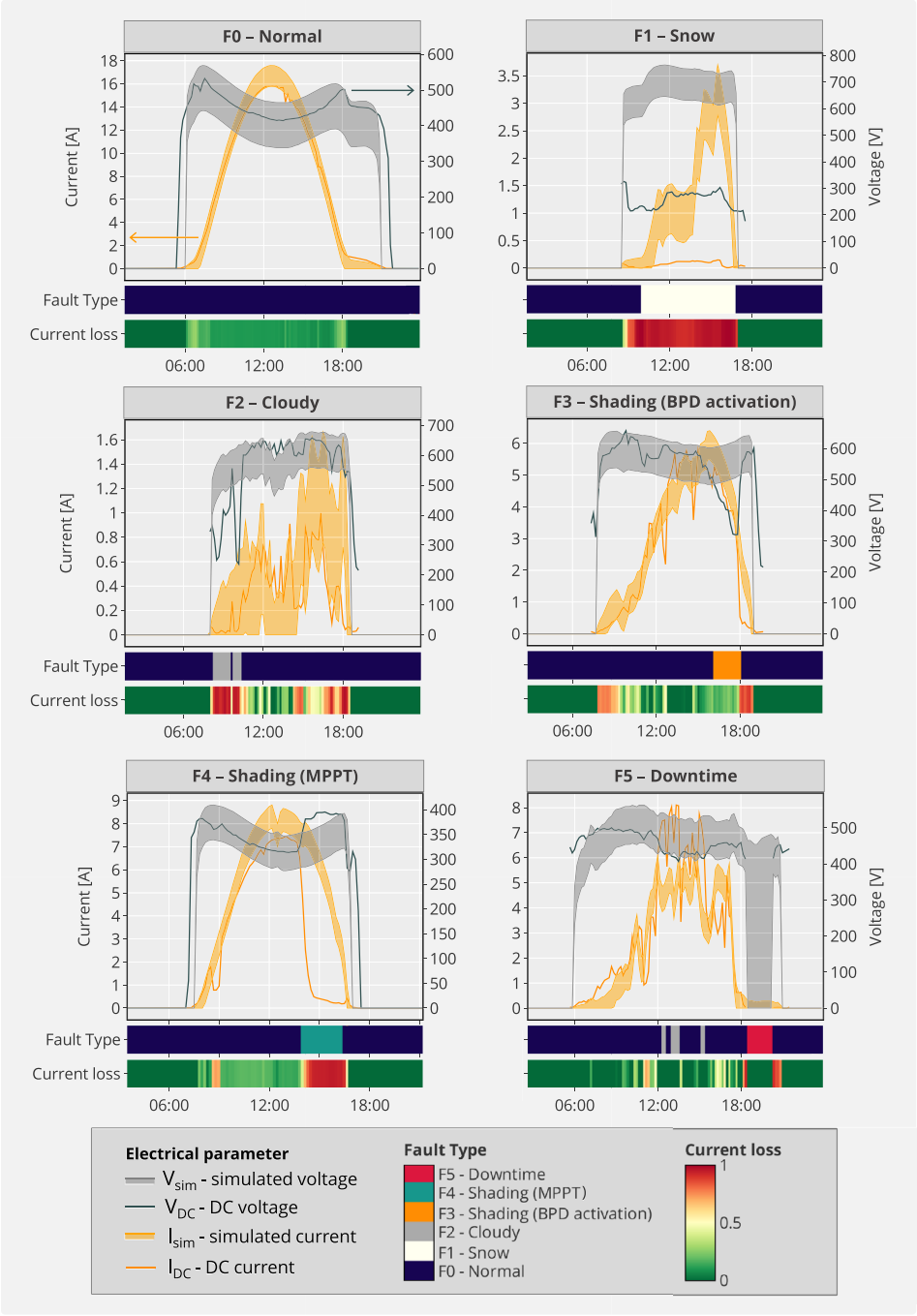

FIGURE 3 Example daily production profiles for the identified loss factors, showing DC voltage and current (solid lines), with simulated thresholds (shaded areas), along with fault type and current loss heat maps. Current and voltage ranges vary due to different systems being used for the example faults. The current loss is computed relative to the simulated output, with values ranging from 0 to 1, where 1 is equivalent to 100% current loss. Used abbreviations: BPD, bypass diode; MPPT, maximum power point tracker.

3.2 | Shaded BIPV system case study: FDD validation

The developed pipeline is applied to a BIPV rooftop system located in the Bern region of Switzerland as a case study and validation for the developed FDDA. The system is east–west oriented, with two 24° tilted roof sides, separated into four strings connected to two inverters. The total system capacity is 21.3 kWp, and this case study will focus on the two west-facing strings of 5.22 kWp capacity each. The system was also analysed on-site to validate the data-based results, with a full system check in August 2022.

Figure 4 shows the FDD analysis resulting heat maps, where colours correspond to the different operating conditions (see Figure 3 for detailed examples of daily production profiles). Yearly heat maps are shown for the system lifetime, highlighting the evolution of LFs over time. The two strings of the roof are analysed separately, with string 1 representing the bottom half of the rooftop and string 2 the top. The following observations are made:

- During all analysed years, morning F4 faults are detected in string 1, corresponding to decreased power output due to partial shading, where a mismatch in the string causes the MPPT

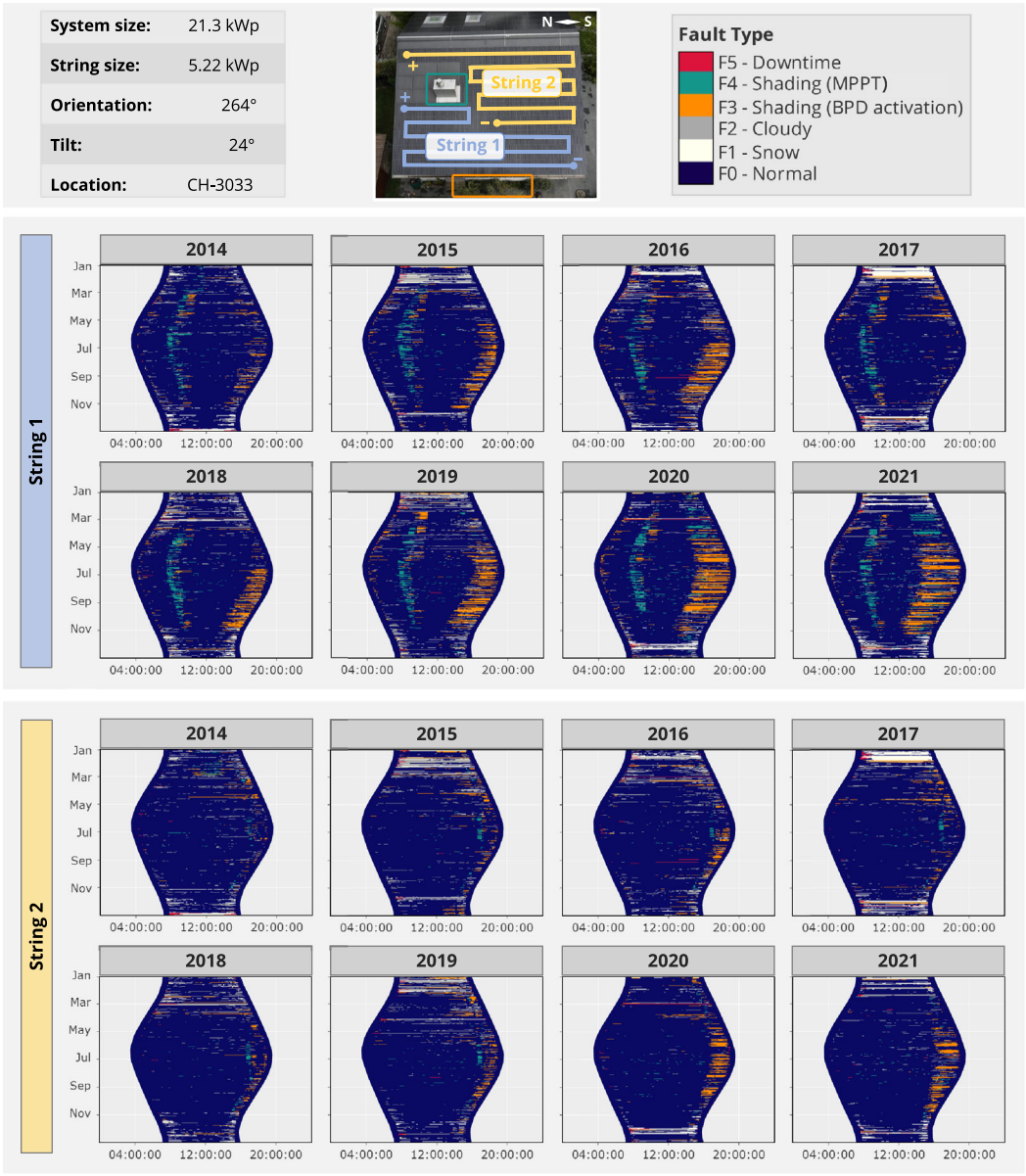

FIGURE 4 Yearly fault type heat maps of the two strings of the west-facing building-integrated PV (BIPV) system rooftop, from 2014 to 2021. Recurring shading events are observed in the morning and evening hours, especially for string 1, due to a chimney and nearby tree. String 2 also sees recurring shading, started from 2019 onwards due to the tree. System information and stringing layout are shown at the top, where the shading elements (chimney and tree) are highlighted in the system photograph.

to function at higher-than-expected voltage and lower current (local MPP identified by the inverter MPPT algorithm). Given the repeating and stable nature of the fault over time, it is likely caused by a permanent shading element. Through on-site analysis of the system, the fault is confirmed to be due to a chimney (highlighted in blue in the roof photograph in Figure 4), which shades modules in the string during morning hours (sun rising from the east).

- Due to the string arrangement, string 2 only shows chimney shading in the evening hours, as the sun sets in the west.
- Recurring BPD activation (F3) is observed for string 1 in the evening hours, with a pattern of increasing intensity over time. The year 2017 is notably unaffected by the fault, which indicates a change in the shading element. Through on-site analysis, the fault is identified as shading from a tree in front of the west-facing roof (highlighted in orange in the roof photograph in Figure 4), which casts a large shadow in afternoon hours.
- With the heavy snow during the 2017 winter (detected in the FDDA as F1 faults), as well as trimming and cutting of branches during that year (confirmed by the PV system owner), the tree was not found to create shadow losses. Notably, the chimney-related shading stress is still observed during that year. From 2018 onward, the tree is seen to shade with increasing intensity, likely linked to the growing branches and foliage.

- String 2 being on the top side of the roof, the tree shading does not cause any recurring BPD activation until 2019, where it starts appearing and increases in the subsequent years. This is attributed to the tree growth, creating a progressively larger shading area and reaching the modules of string 2.
- Looking at string 1 during the year 2021, and considering the shading faults F3 due to the tree, potential yield gains over the year are estimated at ~0.63 MWh/year, representing a potential 10% increase in total string output for that year if the tree were cut down or reduced enough in size to avoid direct shadowing of modules.
- Linking back to Figure 1 with the LFs and DMs, string 1 is found to have at least one broken BPD through the on-site analysis, which is likely directly tied to the recurring shading events, causing heavy thermal and thermomechanical stress in the repeated activation.

The FDD analysis therefore yields important outcomes for both the system owner and installer or manufacturer, leading to the quantification of avoidable losses due to surrounding elements. With this case study, the defined fault types of the FDDA are therefore validated, and the patterns in the heat maps correlate directly to the shading induced by the surrounding elements. Notably, even without on-site confirmation of the shading origin, the fault evolution over time indicates the variable nature of the shadowing elements, which would be enough to suppose an avoidable loss pattern.

3.3 | Shaded BIPV system case study: Long-term performance assessment

The next step in this case study is the long-term performance assessment. Figure 5 shows the resulting PR trends and PLR values for the two analysed strings, distinguishing between the standard PLR and i-PLR. The intrinsic PR trend and i-PLR value are the result of the additional filtering of LFs resulting from the prior FDD step. Comparing both methods highlights the impact of the identified LFs on the long-term performance of the strings. The yearly relative yield losses per fault type are also shown for each string, calculated as the relative difference between the simulated DC power and actual power during time steps where each LF is detected. The following observations are made:

- For string 1, the standard PLR is found to be −1.7%/year, which is higher than the expected −0.5 to −0.75%/year described in literature for crystalline Silicon technology.[77] This could indicate that (i) the system is degrading over time, causing lowering

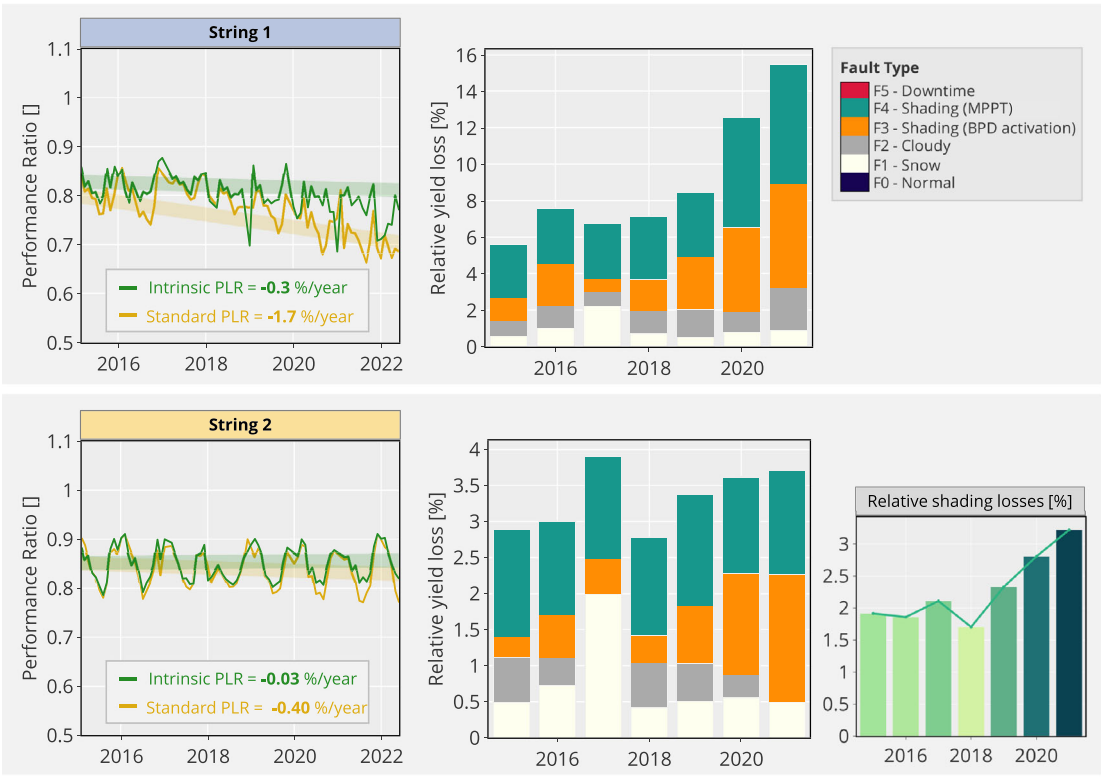

FIGURE 5 (Left) Daily performance ratio trends and reported performance loss rates for standard performance loss rate (PLR) and intrinsic PLR (with fault type filtering, removing the loss factors detected through the fault detection algorithm) for the two analysed building-integrated PV (BIPV) strings. The resulting PLR values are reported in the figure legends, and represented by a solid linear trend line to highlight the difference between the two methods. (Right) Yearly relative yield losses (comparing simulated optimal yield and actual yield) per identified fault type. For string 2, the relative shading losses (isolating F3 and F4) are shown separately to highlight their increase over time.

performance, (ii) the system is experiencing conditions which lead to decreasing yield patterns over time or (iii) a combination of the above, which is the most likely explanation when using the standard PLR computation methods. With the help of the detailed FDDA results, the decoupling of performance loss effects is possible, and the result of this filtering is a median i-PLR of −0.3%/year. The i-PLR is therefore 80% higher compared with the standard method.

- Looking at the relative yield losses over time, shading losses increase by a factor 3 between 2017 and 2021, leading to a drift in the daily PR trend. The increasing shading therefore directly impacts the long-term performance results, creating a bias which is not directly linked to system degradation, but only reversible loss effects.
- String 2 shows good agreement between the PR trends prior to 2018, at which point a progressive increase in shading losses also starts to cause a negative bias. Although the relative losses are minor compared with string 1, the resulting standard PLR is still higher than the i-PLR, which shows almost no change in performance when looking at the system in normal operating conditions (filtering all detected LFs).

Figure 6 shows the exact PLR values and the CIs resulting from the statistical method. The CIs show that the difference between the PLR and i-PLR is statistically significant. Interestingly, string 1 still sees significant i-PLR (around −0.3%/year), while the i-PLR for string 2 is close to zero. This indicates that most of the performance losses observed in the standard PLR for string 2 are likely due to reversible LFs, and the intrinsic system health is stable over the study period.

This case study highlights (i) the importance of understanding the PLR value and how it is not a quantification of degradation but rather an indicator of the overall system performance and (ii) that LF analysis and FDD should be used in tandem with long-term performance assessments to decouple these effects, giving a better reflection of actual system health rather than system output performance.

3.4 | Fleet analysis: Loss patterns and i-PLR bias

Having seen examples of the FDDA results for a specific case study, it is interesting to expand the results to a fleet of systems. A total of 250+ individual strings were analysed, from 60+ BIPV and BAPV systems in Switzerland. After data cleaning and processing, results are obtained for 54 systems, corresponding to 160 strings. The goal here is to determine the different types of biases caused by the reversible faults categorised through the FDDA. Future work will focus on applying the full pipeline to larger fleets of systems and extracting relevant performance statistics.

Given the observations from the case study, the results for the fleet of systems are therefore used to distinguish the impact of LFs on the PLR, with a focus on partial shading, which is especially relevant to PV systems in the built environment. To do so, the FDDA and PLR pipelines are applied to all 160 strings, and the i-PLR is compared with the PLR along with the evolution of estimated shading losses over time. The results of this analysis yielded four categories of losses or four typical patterns of PLR bias due to the influence of evolving shading losses in time. Figure 7 shows the results for four representative BIPV strings, selected for each category. The standard and i-PLR

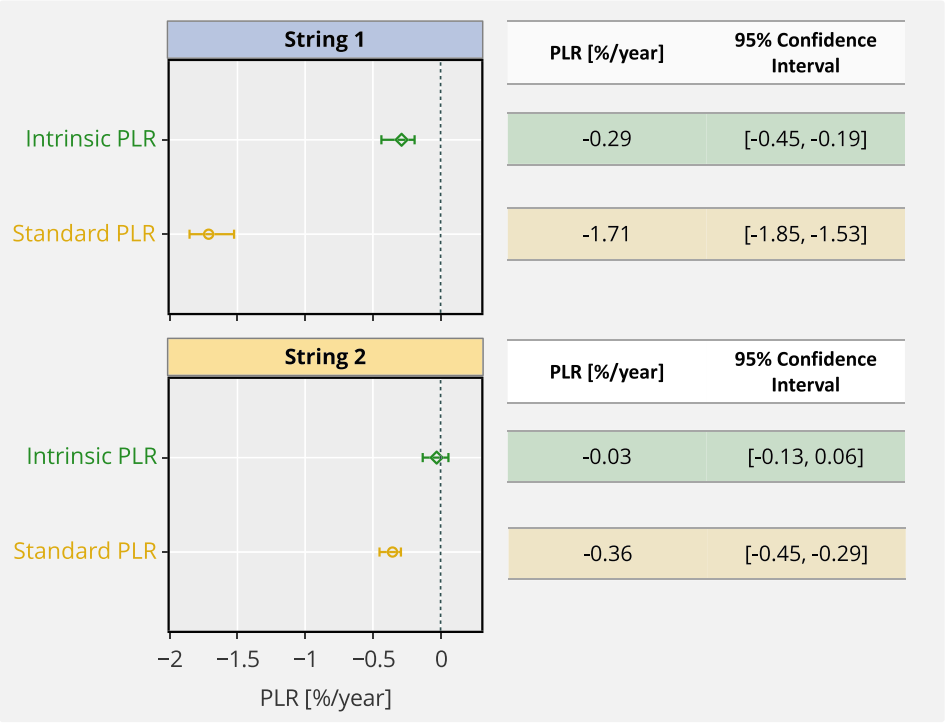

	PLR [%/year]	95% Confidence Interval
Intrinsic PLR	-0.29	[-0.45, -0.19]
Standard PLR	-1.71	[-1.85, -1.53]

	PLR [%/year]	95% Confidence Interval
Intrinsic PLR	-0.03	[-0.13, 0.06]
Standard PLR	-0.36	[-0.45, -0.29]

FIGURE 6 Standard and intrinsic performance loss rate (PLR) values for the two case study strings. (Left) median PLR values and confidence interval (CIs). (Right) table reporting the PLR results and CIs.

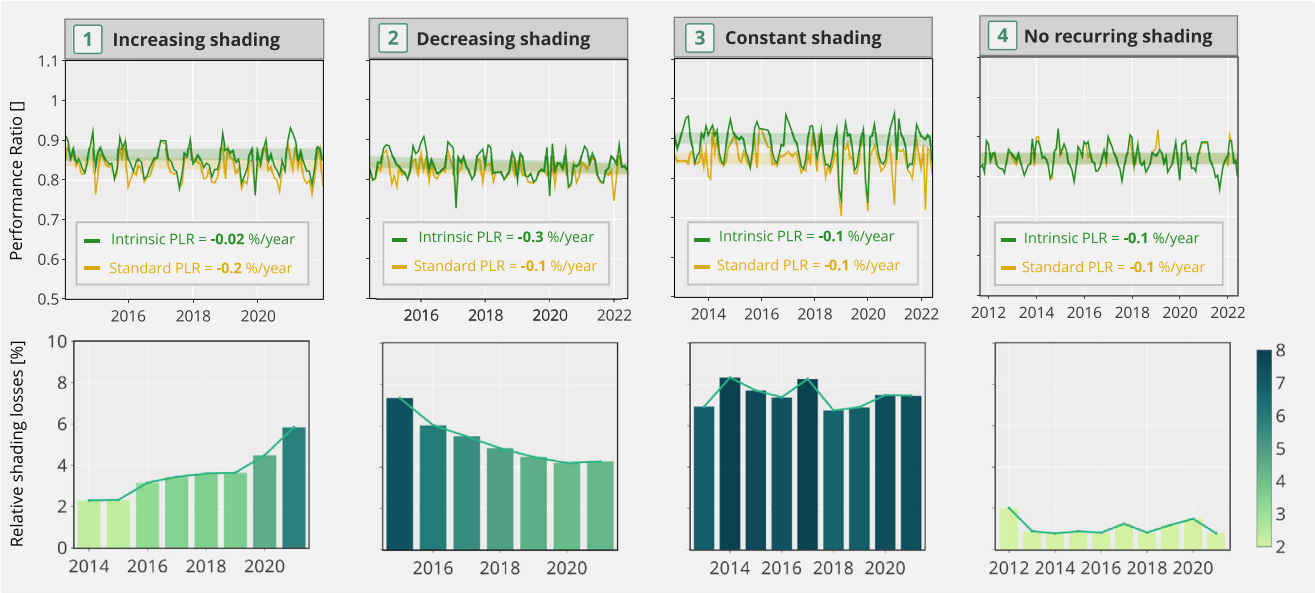

FIGURE 7 Comparison of daily performance ratio (PR) trends for the intrinsic and standard performance loss rates (PLRs) for the four identified shading loss scenarios (exemplified with different building-integrated PV [BIPV] systems), highlighting the potential shift in PR after filtering for loss factors and the impact on the PLR evaluation. Corresponding yearly relative shading loss evolution is also shown.

values are compared, with the corresponding PR trends, as well as the evolution of relative shading losses in time. The main loss and bias patterns are categorised as follows:

1. **Increasing shading:** when shading losses increase over time, the standard PLR is negatively biassed and shows higher values than the i-PLR due to the down shift in PR. This results in an overestimation of the PV string performance degradation.
2. **Decreasing shading:** when shading losses decrease over time, the standard PLR is positively biassed and shows lower values than the i-PLR due to the up shift in PR. This results in an underestimation of the PV string performance degradation.
3. **Constant shading:** when shading losses do not vary over time, the standard and i-PLR are the same, as there is a constant shift in PR trends.
4. **No recurring shading:** when there are no or very low shading losses over time, the standard and i-PLR are the same and there is no shift in PR trends.

4 | DISCUSSION

The definition of the i-PLR and the developed methodology combining FDD and PLR assessments into one analysis pipeline were shown to successfully decouple the reversible losses, which are also quantified, from the PV system degradation. The following discussion will go through the scientific innovations of the proposed method, as well as the caveats and limitations.

4.1 | Scientific impact and innovations

- The combination of fault detection methods with long-term performance data analytics brings many interesting insights regarding the reliability of PV systems. The double approach enables the decoupling of intrinsic and extrinsic performance loss effects, which has been highlighted in recent works as an important research area for PV system reliability.[22,23] The results highlight the importance of taking into account LFs when analysing PV system data, as they can cause significant biases in the final PLR value.
- The defined i-PLR metric is therefore a reflection of module degradation, although it still accounts for other system components degradation. Consequently, it serves as valuable information for installers and O&M companies in relation to contractual guarantees and module warranties. The FDD outputs may hold significant relevance for optimising O&M procedures, facilitating the transition from reactive/preventative maintenance to a predictive maintenance approach. With strong potential savings in O&M costs, this solution can help increase the reliability and profitability of PV projects.[78]
- This work also highlights the importance of a correct definition of performance metrics in the PV reliability field. The standard PLR is still a useful and informative metric; however, its scope is often misrepresented in literature and in industry applications. The i-PLR defined here can be considered a step closer to the quantification of system degradation, although this value should still not be confused with module-level degradation.
- The results presented in this work have a unique focus on small-scale PV systems in the built environment. Various studies have

already reported utility-scale systems performance,[24,37] but such findings may not be readily applied to small systems,[45] where the definition of the i-PLR is particularly relevant given the prevalence of shading faults, which are seen to have a high impact on the PLR.

- Focusing on small-scale PV systems also allows for higher granularity in the treatment of data—the developed algorithms and analysis methods can be applied on a string-level (e.g. 20 modules connected in series), as opposed to the typical system-level approach most common in literature. This adds valuable insights in the observed mismatches in performance and allows for more detailed and effective classification of defects. In large-scale PV installations, the use of central inverters typically reduces data granularity, leading to the overlapping of LFs and DMs.

4.2 | Limitations and future work

- The current work is only applied to BIPV and BAPV systems, although the methodology is not limited to any particular system configuration. The input requirements are simply the DC system outputs and satellite or ground-based weather data. In general, small-scale systems will benefit from higher data granularity but lack on-site meteorological data monitoring, while utility-scale systems are often equipped with pyranometers or weather stations but tend to have low spatial granularity in terms of inverter data. There is therefore a trade-off between the precision of FDD and uncertainty of performance trend: Results of the FDD analysis will typically be more detailed for small-scale systems, as there can be superposition of DMs for larger installations. However, uncertainty linked to solar resource inputs may be lower for larger systems, which can impact the assessment of the PLR.
- The identified LFs do not cover all potential reversible loss effects. Extensions could include soiling, which is a reversible fault causing bias in the PV system data.[37] The main limitation in the case of soiling is that the losses do not manifest in a finite time step with specific DC output fingerprints; the losses are progressive, affecting mainly the current, and are often too low to be able to quantify accurately without soiling sensors. A potential way around the soiling impact in system performance is to filter for clear-sky days that occur after precipitation events, which would minimise the impact of soiling accumulation.
- There are many sources of uncertainty in the analysis pipeline, which compound and transfer to the final PLR value: measurement uncertainties related to the inverters and meteorological data sources (high for satellite-based), uncertainties in the fault detection and statistical thresholds, errors in the performance metric (PR) and statistical uncertainty in the PLR calculation (here the YoY method). Minimising these uncertainties will be the focus of future work.
- Climate and technology have also been shown to impact the accuracy and uncertainty of PLR assessments.[79] The proposed method in this work, namely, the inclusion of fault detection steps in the PLR analysis pipeline, is in theory climate- and technology-independent. Specifically, the concept of filtering reversible losses from PV system data should be independent of the system location or module type. Nevertheless, given that the YoY statistical method is used to compute the PLR and that this method has been shown to be biassed in certain climates, future work should examine the sensitivity of the i-PLR in various conditions (e.g. using synthetic data with induced faults and PLR for various technologies and climates).
- Although the i-PLR is a better reflection of the DMs affecting the PV system and therefore arguably serves as a better representation of system reliability linked to the manufacturer's warranty, it is still not to be confused with module-level degradation and includes all system and electrical losses.

5 | CONCLUSION

This work is a first attempt to bridge the gap between the fields of FDD and PLRs in PV systems. Reversible LFs, which impact short-term PV system performance, are shown to impact and bias the PLR evaluation of PV systems. The developed fault detection method is shown to successfully identify partial shading, snow and downtime losses in a case study with on-site validation, where evolving yield losses over time led to a shift in PR trend. This approach may be extended to further identify, classify and filter other LF (e.g. soiling). Furthermore, a fleet analysis of PV systems in the built environment enabled the identification of four distinct PLR bias patterns associated with changes in yield losses over time. While the presented results are specific to BIPV and BAPV systems, the combined FDD and PLR pipeline is applicable to all PV system configurations, and future work will examine larger PV system fleets with varying configurations and capacities. Overall, the introduction of the newly defined i-PLR, with the additional filtering of reversible losses, provides a more accurate reflection of PV system health and reliability compared with the standard PLR. Future work in the field should therefore consider integrating such filtering steps in order to improve accuracy in performance assessments and avoid erroneous interpretations of the PLR. Additionally, further research should address the limitations of the presented work, such as improving the coverage of identified LFs and minimising the sources of uncertainty in the analysis pipeline.

ACKNOWLEDGEMENTS

The authors acknowledge the financial support from the Swiss Federal Office of Energy (SFOE) through the ASSURed PV project (contract 502408-01). The authors thank Solcast for the use of their satellite-derived meteorological data. The authors would like to express their gratitude to Andrew Fairbrother for his assistance in laying the groundwork for the Fault Detection and Diagnosis analysis and providing access to the necessary data. Finally, the authors thank Pascal Müller, Philipp Wälchli, Nicolas Wyrsch and Alejandro Pena Bello for the fruitful discussions. Open access funding provided by Ecole Polytechnique Federale de Lausanne.

DATA AVAILABILITY STATEMENT

The data that support the findings of this study are available on request from the corresponding author. The data are not publicly available due to privacy or ethical restrictions.

ORCID

Hugo Quest https://orcid.org/0000-0003-3945-3093

REFERENCES

1. Haegel NM, Verlinden P, Victoria M, et al. Photovoltaics at multi-terawatt scale: waiting is not an option. *Science*. 2023;380(6640):39-42. doi:10.1126/science.adf6957
2. SolarPower Europe. Global market outlook for solar power 2022-2026. Technical report, 2022. URL https://www.solarpowereurope.org/insights/market-outlooks/global-market-outlook-for-solar-power-2022.
3. Haegel NM, Atwater H, Barnes T, et al. Terawatt-scale photovoltaics: transform global energy. *Science*. 2019;364(6443):836-838. doi:10.1126/science.aaw1845
4. SolarPower Europe. Global market outlook for solar power 2023-2027. Technical report, 2023. URL https://www.solarpowereurope.org/insights/outlooks/global-market-outlook-for-solar-power-2023-2027.
5. Verlinden P. Future challenges for photovoltaic manufacturing at the terawatt level. *Journal of Renewable and Sustainable Energy*. 2020;12(5):053505. doi:10.1063/5.0020380
6. Fan F, Li J, Yang TC-J, et al. Monolithic perovskite-silicon tandem solar cells: from the lab to fab? *Adv Mater*. 2022. ISSN 1521-4095;34(24):2106540. doi:10.1002/adma.202106540
7. Ballif C, Haug F-J, Boccard M, Verlinden PJ, Hahn G. Status and perspectives of crystalline silicon photovoltaics in research and industry. *Nat Rev Mater*. 2022. ISSN 2058-8437;7(8):597-616. doi:10.1038/s41578-022-00423-2
8. Allouhi A, Rehman S. Mahmut Sami Buker, and Zafar Said. Up-to-date literature review on solar PV systems: technology progress, market status and R&D. *J Clean Prod*. 2022. ISSN 0959-6526;362:132339. doi:10.1016/j.jclepro.2022.132339
9. Siegler TD, Dawson A, Lobaccaro P, et al. The path to perovskite commercialization: a perspective from the United States solar energy technologies office. *ACS Energy Let*. 2022;7(5):1728-1734. doi:10.1021/acsenergylett.2c00698
10. Arruti OA, Virtuani A, Ballif C. Long-term performance and reliability of silicon heterojunction solar modules. *Progr Photovolt: Res Appl*. 2023. ISSN 1099-159X;31(7):664-677. doi:10.1002/pip.3688
11. Aghaei M, Fairbrother A, Gok A, et al. Review of degradation and failure phenomena in photovoltaic modules. *Renew Sustain Energy Rev*. 2022. ISSN 1364-0321;159:112160. doi:10.1016/j.rser.2022.112160
12. Aslam A, Ahmed N, Qureshi SA, Assadi M, Ahmed N. Advances in solar PV systems: a comprehensive review of PV performance, influencing factors, and mitigation techniques. *Energies*. 2022. ISSN 1996-1073;15(20):7595. doi:10.3390/en15207595
13. Kettle J, Aghaei M, Ahmad S, et al. Review of technology specific degradation in crystalline silicon, cadmium telluride, copper indium gallium selenide, dye sensitised, organic and perovskite solar cells in photovoltaic modules: understanding how reliability improvements in mature technologies can enhance emerging technologies. *Progr Photovolt: Res Appl*. 2022. ISSN 1099-159X;30(12):1365-1392. doi:10.1002/pip.3577
14. Kim J, Rabelo M, Padi SP, Yousuf H, Cho E-C, Yi J. A review of the degradation of photovoltaic modules for life expectancy. *Energies*. 2021. ISSN 1996-1073;14(14):4278. doi:10.3390/en14144278
15. Dhimish M, Mather P, Holmes V. Evaluating power loss and performance ratio of hot-spotted photovoltaic modules. *IEEE Transactions on Electron Devices*. 2018. ISSN 1557-9646; Conference name: IEEE transactions on electron devices65(12):5419-5427. doi:10.1109/TED.2018.2877806
16. Schweiger M, Herrmann W, Gerber A, Rau U. Understanding the energy yield of photovoltaic modules in different climates by linear performance loss analysis of the module performance ratio. *IET Renew Power Gen*. 2017. ISSN 1752-1424;11(5):558-565. doi:10.1049/iet-rpg.2016.0682
17. Quansah DA, Adaramola MS. Assessment of early degradation and performance loss in five co-located solar photovoltaic module technologies installed in Ghana using performance ratio time-series regression. *Renew Energy*. 2019. ISSN 0960-1481;131:900-910. doi:10.1016/j.renene.2018.07.117
18. Makrides G, Zinsser B, Schubert M, Georghiou GE. Performance loss rate of twelve photovoltaic technologies under field conditions using statistical techniques. *Solar Energy*. 2014. ISSN 0038-092X;103:28-42. doi:10.1016/j.solener.2014.02.011
19. Virtuani A, Caccivio M, Annigoni E, et al. 35 years of photovoltaics: analysis of the TISO-10-kW solar plant, lessons learnt in safety and performance—part 1. *Progr Photovolt: Res Appl*. 2019. ISSN 1099-159X;27(4):328-339. doi:10.1002/pip.3104
20. Annigoni E, Virtuani A, Caccivio M, Friesen G, Chianese D, Ballif C. 35 years of photovoltaics: analysis of the TISO-10-kW solar plant, lessons learnt in safety and performance—part 2. *Progr Photovolt: Res Appl*. 2019. ISSN 1099-159X;27(9):760-778. doi:10.1002/pip.3146
21. French RH, Bruckman LS, Moser D, et al. Assessment of performance loss rate of PV power systems. *Technical Report Report* IEA-PVPS T13–22:2021. 2021. ISBN: 978–3–907281-10-9. https://iea-pvps.org/key-topics/assessment-of-performance-loss-rate-of-pv-power-systems/
22. Lindig S, Theristis M, Moser D. Best practices for photovoltaic performance loss rate calculations. *Progr Energy*. 2022. ISSN 2516–1083;4(2):022003. doi:10.1088/2516-1083/ac655f
23. Deceglie MG, Anderson K, Fregosi D, et al. Perspective: performance loss rate in photovoltaic systems. *Solar RRL*. 2023. ISSN 2367-198X;7(15):2300196. doi:10.1002/solr.202300196
24. Lindig S, Moser D, Curran AJ, et al. International collaboration framework for the calculation of performance loss rates: data quality, benchmarks, and trends (towards a uniform methodology). *Progr Photovolt: Res Appl*. 2021. ISSN 1099-159X;29(6):573-602. doi:10.1002/pip.3397
25. Phinikarides Alexander, Kindyni Nitsa, Makrides George, and Georghiou George E.. Review of photovoltaic degradation rate methodologies. *Renew Sustain Energy Rev*, 40: 143–152, 2014. ISSN 1364-0321. 10.1016/j.rser.2014.07.155. URL https://www.sciencedirect.com/science/article/pii/S1364032114006078.
26. Romero-Fiances I, Livera A, Theristis M, et al. Impact of duration and missing data on the long-term photovoltaic degradation rate estimation. *Renew Energy*. 2022. ISSN 0960-1481;181:738-748. doi:10.1016/j.renene.2021.09.078
27. Jordan DC, Deline C, Kurtz SR, Kimball GM, Anderson M. Robust PV degradation methodology and application. *IEEE J Photovolt*. 2018. ISSN 2156-3403;8(2):525-531. doi:10.1109/JPHOTOV.2017.2779779
28. Hasselbrink E, Anderson M, Defreitas Z, Mikofski M, Shen Y-C, Caldwell S, Terao A, Kavulak D, Campeau Z, DeGraaff D. Validation of the PVLife model using 3 million module-years of live site data. In 2013 IEEE 39th Photovoltaic Specialists Conference (PVSC), pages 0007–0012, 2013. 10.1109/PVSC.2013.6744087.
29. Decelgie Michael, Nag Ambarish, Shinn Adam, Kimball Gregory, Ruth Daniel, Jordan Dirk, Yang Jiyang, Anderson Kevin, Perry Kirsten, Mikofski Mark, Muller Matthew, Vining Will, and Deline Chris.

RdTools, version 2.1.8, computer software. 2023. 10.5281/zenodo.10150362.
30. Cleveland RB, Cleveland WS, Terpenning I. STL: a seasonal-trend decomposition procedure based on loess. *J Off Statistics*. 1990;6(1):3. ISSN 0282423X.
31. Meyers B. *Michaelangelo Tabone, and Emre Can Kara*. Statistical Clear Sky Fitting Algorithm; 2019.
32. Meyers B, Deceglie M, Deline C, Jordan D. Signal processing on PV time-series data: robust degradation analysis without physical models. *IEEE J Photovolt*. 2020. ISSN 2156-3403;10(2):546-553. doi:10.1109/JPHOTOV.2019.2957646
33. Livera A, Theristis M, Makrides G, Sutterlueti J, Ransome S, Georghiou G. Performance analysis of mechanistic and machine learning models for photovoltaic energy yield prediction. 2019.
34. Theristis Marios, Andreas Livera, Birk Jones C., Makrides George, Georghiou George E., and Stein Joshua S.. Nonlinear photovoltaic degradation rates: modeling and comparison against conventional methods. *IEEE J Photovolt*, 2020. ISSN 2156-3403. Conference Name: IEEE Journal of Photovoltaics, 10, 4, 1112-1118, doi:10.1109/JPHOTOV.2020.2992432.
35. Lindig S, Louwen A, Moser D, Topic M. New PV performance loss methodology applying a self-regulated multistep algorithm. *IEEE J Photovolt*. 2021;11(4):1087-1096. doi:10.1109/JPHOTOV.2021.3078075
36. Theristis M, Livera A, Micheli L, et al. Comparative analysis of change-point techniques for nonlinear photovoltaic performance degradation rate estimations. *IEEE J Photovolt*. 2021. ISSN 2156-3403;11(6):1511-1518. doi:10.1109/JPHOTOV.2021.3112037
37. Livera A, Theristis M, Micheli L, Stein JS, Georghiou GE. Failure diagnosis and trend-based performance losses routines for the detection and classification of incidents in large-scale photovoltaic systems. *Progr Photovolt: Res Appl*. 2022. ISSN 1099-159X;30(8):921-937. doi:10.1002/pip.3578
38. de Oliveira AKV, Aghaei M, Rüther R. Automatic inspection of photovoltaic power plants using aerial infrared thermography: a review. *Energies*. 2055;15(6):2022. ISSN 1996-1073. doi:10.3390/en15062055
39. Verma K, Gawre SK, Kumar S. Comparison between novel fault detection techniques in solar PV arrays: a review. In: Gupta OH, Sood VK, Malik OP, eds. *Recent Advances in Power Systems: Select Proceedings of EPREC-2021, Lecture Notes in Electrical Engineering*. Springer Nature; 2022. ISBN 9789811669705:27-37. doi:10.1007/978-981-16-6970-5_3
40. Gaviria JF, Narváez G, Guillen C, Giraldo LF, Bressan M. Machine learning in photovoltaic systems: a review. *Renew Energy*. 2022. ISSN 0960–1481;196:298-318. doi:10.1016/j.renene.2022.06.105
41. Malik A, Haque A, Kurukuru VSB, Khan MA, Blaabjerg F. Overview of fault detection approaches for grid connected photovoltaic inverters. *e-Prime – Adv Electr Eng Electron Energy*. 2022. ISSN 2772-6711;2:100035. doi:10.1016/j.prime.2022.100035
42. Hong Y-Y, Pula RA. Methods of photovoltaic fault detection and classification: a review. *Energy Rep*. 2022. ISSN 2352-4847;8:5898-5929. doi:10.1016/j.egyr.2022.04.043
43. Koester L, Lindig S, Louwen A, Astigarraga A, Manzolini G, Moser D. Review of photovoltaic module degradation, field inspection techniques and techno-economic assessment. *Renew Sustain Energy Rev*. 2022. ISSN 1364-0321;165:112616. doi:10.1016/j.rser.2022.112616
44. Aghaei M. Autonomous monitoring and analysis of photovoltaic systems. *Energies*. 2022;15(14):5011. doi:10.3390/en15145011
45. Fairbrother A, Quest H, Özkalay E, et al. Long-term performance and shade detection in building integrated photovoltaic systems. *Solar RRL*. 2022. ISSN 2367-198X;6(5):2100583. doi:10.1002/solr.202100583
46. Tati F, Talhaoui H, Aissa O, Dahbi A. Intelligent shading fault detection in a PV system with MPPT control using neural network technique. *Int J Energy Environ Eng*. 2022. ISSN 2251-6832;13(4):1147-1161. doi:10.1007/s40095-022-00486-5
47. Liu J, Wang M, Curran AJ, et al. Degradation mechanisms and partial shading of glass-backsheet and double-glass photovoltaic modules in three climate zones determined by remote monitoring of time-series current–voltage and power datastreams. *Solar Energy*. 2021. ISSN 0038-092X;224:1291-1301. doi:10.1016/j.solener.2021.06.022
48. Tsafarakis O, Sinapis K, van Sark W. A time-series data analysis methodology for effective monitoring of partially shaded photovoltaic systems. *Energies*. 2019;12(9):1722. doi:10.3390/en12091722
49. Köntges M, Kurtz S, Packard C, et al. *Performance and Reliability of Photovoltaic Systems: Subtask 3.2: Review of Failures of Photovoltaic Modules: IEA PVPS task 13: External Final Report IEA-PVPS*. International Energy Agency, Photovoltaic Power Systems Programme; 2014. ISBN 978–3–906042-16-9
50. Drif M, Mellit A, Aguilera J, Pérez PJ. A comprehensive method for estimating energy losses due to shading of GC-BIPV systems using monitoring data. *Solar Energy*. 2012. ISSN 0038-092X;86(9):2397-2404. doi:10.1016/j.solener.2012.05.008
51. Norton B, Eames PC, Mallick TK, et al. Enhancing the performance of building integrated photovoltaics. *Solar Energy*. 2011. ISSN 0038-092X;85(8):1629-1664. doi:10.1016/j.solener.2009.10.004
52. Fouad MM, Shihata LA, Morgan ESI. An integrated review of factors influencing the perfomance of photovoltaic panels. *Renew Sustain Energy Rev*. 2017. ISSN 1364-0321;80:1499-1511. doi:10.1016/j.rser.2017.05.141
53. Kempe MD, Holsapple D, Whitfield K, Shiradkar N. Standards development for modules in high temperature micro-environments. *Progr Photovolt: Res Appl*. 2021. ISSN 1099-159X;29(4):445-460. doi:10.1002/pip.3389
54. IEC. IEC TS 63126:2020 - Guidelines for qualifying PV modules, components and materials for operation at high temperatures, 2020. URL https://standards.iteh.ai/catalog/standards/iec/e5b0df77-3a3c-497c-9a18-82341bfe7ba7/iec-ts-63126-2020.
55. Dhere NG, Shiradkar N, Schneller E, Gade V. The reliability of bypass diodes in PV modules. In: *Reliability of Photovoltaic Cells, Modules, Components, and Systems VI*. International Society for Optics and Photonics; 2013. doi:10.1117/12.2026782
56. Dolara Alberto, Lazaroiu George Cristian, and Ogliari Emanuele. Efficiency Analysis of PV Power Plants Shaded by MV Overhead Lines. *Int J Energy Environ Eng*, 7 (2): 115–123, 2016. ISSN 2251-6832. 10.1007/s40095-016-0208-2.
57. Özkalay E, Valoti F, Caccivio M, Virtuani A, Friesen G, Ballif C. The effect of partial shading on the reliability of photovoltaic modules in the built-environment, 2023. [Unpublished manuscript].
58. Ghosh A. Potential of building integrated and attached/applied photovoltaic (BIPV/BAPV) for adaptive less energy-hungry building's skin: a comprehensive review. *J Clean Prod*. 2020. ISSN 0959-6526;276:123343. doi:10.1016/j.jclepro.2020.123343
59. Liu Z, Zhang Y, Yuan X, et al. A comprehensive study of feasibility and applicability of building integrated photovoltaic (BIPV) systems in regions with high solar irradiance. *J Clean Prod*. 2021. ISSN 0959-6526;307:127240. doi:10.1016/j.jclepro.2021.127240
60. Virtuani A, Block AB, Wyrsch N, Ballif C. The carbon intensity of integrated photovoltaics. *Joule*. 2023. ISSN 2542–4351; Publisher: Cell Press7(11):2511-2536. doi:10.1016/j.joule.2023.09.010
61. Fairbrother A, Virtuani A, Ballif C. Outdoor operating temperature of modules in BIPV and BAPV topologies. *37th European Photovoltaic Solar Energy Conference and Exhibition*, pages 1752–1756, 2020. 10.4229/EUPVSEC20202020-6DO.13.3.

62. Özkalay E, Friesen G, Caccivio M, et al. Operating temperatures and diurnal temperature variations of modules installed in open-rack and typical BIPV configurations. *IEEE J Photovolt*. 2022. ISSN 2156-3403; 12(1):133-140. doi:10.1109/JPHOTOV.2021.3114988
63. Gok A, Özkalay E, Friesen G, Frontini F. The influence of operating temperature on the performance of BIPV modules. *IEEE J Photovolt*. 2020. ISSN 2156-3403;10(5):1371-1378. doi:10.1109/JPHOTOV.2020.3001181
64. Al Mamun MA, Hasanuzzaman M, Selvaraj J. Experimental investigation of the effect of partial shading on photovoltaic performance. *IET Renew Power Gen*. 2017. Publisher: IET Digital Library;11(7):912-921. doi:10.1049/iet-rpg.2016.0902
65. Jensen Adam R., Anderson Kevin S., Holmgren William F., Mikofski Mark A., Hansen Clifford W., Boeman Leland J., and Loonen Roel. pvlib iotools—open-source python functions for seamless access to solar irradiance data. *Solar Energy*, 266: 112092, 2023. ISSN 0038-092X. 10.1016/j.solener.2023.112092. URL https://www.sciencedirect.com/science/article/pii/S0038092X23007260.
66. Loutzenhiser PG, Manz H, Felsmann C, Strachan PA, Frank T, Maxwell GM. Empirical validation of models to compute solar irradiance on inclined surfaces for building energy simulation. *Solar Energy*. 2007. ISSN 0038-092X;81(2):254-267. doi:10.1016/j.solener.2006.03.009
67. Holmgren WF, Hansen CW, Mikofski MA. pvlib python: a python package for modeling solar energy systems. *J Open Source Softw*. 2018. ISSN 2475-9066;3(29):884. doi:10.21105/joss.00884
68. Kratochvil Jay A., Boyson William Earl, and King David L.. *Photovoltaic Array Performance Model. Technical Report SAND2004-3535*, Sandia National Laboratories (SNL), 2004. URL https://www.osti.gov/biblio/919131/.
69. Quest H, Fairbrother A, Müller P, Ballif C, Virtuani A. Solar irradiance classification for improved PV performance assessments. 2022. 10.13140/RG.2.2.16943.82085.
70. Livera A, Theristis M, Koubli E, et al. Data processing and quality verification for improved photovoltaic performance and reliability analytics. *Progr Photovolt Res Appl*. 2020;29(2):1-16. doi:10.1002/pip.3349
71. Lindig S, Louwen A, Moser D, Topic M. Outdoor PV system monitoring—input data quality, data imputation and filtering approaches. *Energies*. 2020;13(19):5099. doi:10.3390/en13195099
72. Lindig S, Ascencio-Vasquez J, Leloux J, Moser D, Topic M. Climate related dependence of performance losses of over (3,500) PV systems. 2020. 10.4229/EUPVSEC20202020-5CV.3.37.
73. Lindig S, Ascencio-Vasquez J, Leloux J, Moser D, Reinders A. Performance analysis and degradation of a large fleet of PV systems. *IEEE J Photovolt*. 2021;11(5):1312-1318. doi:10.1109/JPHOTOV.2021.3093049
74. Jordan DC, Deceglie MG, Kurtz SR. PV degradation methodology comparison—a basis for a standard. In 2016 IEEE 43rd photovoltaic specialists conference (PVSC), pages 0273–0278, June 2016. 10.1109/PVSC.2016.7749593.
75. Özkalay E, Virtuani A, Fairbrother A, Skoczek A, Friesen G, Ballif C. Quantifying performance loss rates of photovoltaic modules using ground-based vs satellite-based meteorological data. 2021. 10.4229/EUPVSEC20212021-5DO.2.1.
76. Quest H, Ballif C, Virtuani A. Towards a robust performance loss rate estimate: minimising the uncertainty in the analysis of photovoltaic system degradation. 2023. 10.4229/EUPVSEC2023/4CV.1.14.
77. Jordan D, Anderson K, Perry K, et al. Photovoltaic fleet degradation insights. *Progr Photovolt: Res Appl*. 2022;30(10):1166-1175. doi:10.1002/pip.3566
78. Virtuani A, Morganti L. Profitability of solar photovoltaic projects: a sensitivity analysis of performance loss curves and operation and maintenance expenses. *Solar RRL*. 2023. ISSN 2367-198X;7(8): 2200663. doi:10.1002/solr.202200663
79. Theristis M, Anderson K, Ascencio-Vasquez J, Stein JS. How climate and data quality impact photovoltaic performance loss rate estimations. *Solar RRL*. 2024. ISSN 2367-198X;8(2):2300815. doi:10.1002/solr.202300815

How to cite this article: Quest H, Ballif C, Virtuani A. Intrinsic performance loss rate: Decoupling reversible and irreversible losses for an improved assessment of photovoltaic system performance. *Prog Photovolt Res Appl*. 2024;1-16. doi:10.1002/pip.3829

APPENDIX A: KEY DEFINITIONS

As highlighted throughout this work, clear definitions of metrics are vital in the understanding of performance loss effects in PV systems, as there is often confusion surrounding performance loss and degradation rates. The following key definitions are presented to solidify all of the main concepts:

- **Loss factor (LF):** transient and reversible effects that cause power loss in PV modules or systems due to external factors. Examples of such factors include partial shading, snow and soiling.
- **Degradation mode (DM):** permanent and irreversible effects that lead to a loss of performance in PV modules or systems due to the degradation of internal components. Examples of such degradation include cell cracks, delamination and glass breakage.
- **Performance ratio (PR):** metric used to assess the performance of a PV module or system, defined in the IEC 61724-1 as the quotient between the system's final yield and its reference yield (see Equation (1)). The Performance Ratio takes into account various factors that can affect the performance, including losses due to shading, soiling, temperature variations (the temperature-corrected PR can solve this) and other environmental and operational conditions. In this work, the system-level standard PR is used.
- **Degradation rate (Rd):** rate of annual decrease in a PV module's performance, expressed as a percentage of the original efficiency lost. This reduction reflects irreversible material degradation due to the cumulative impact of various factors, including environmental conditions, damage to module components and the effects of long-term wear and tear, that is, the module-level DMs. The degradation rate does not encompass system-level losses or reversible loss factors, and exclusively addresses module-level degradation. Therefore, at the system-level, the degradation rate represents the average module degradation across the PV array.
- **Performance loss rate (PLR):** metric used to quantify the annual reduction in PV module or system performance, defined as the

change in annualised performance ratio relative to the first year of operation (see Equation (3)). The PLR includes both the reversible loss factors (e.g. shading and snow) and irreversible DMs (e.g. cell cracks and delamination).

- **Intrinsic performance loss rate (i-PLR):** adjusted PLR metric, where loss factors causing reversible losses are filtered out using a fault detection and diagnosis algorithm, therefore reflecting the intrinsic system losses and DMs.